Am J Cancer Res 2024;14(6):3059-3067
www.ajcr.us /ISSN:2156-6976/ajcr0156885

Original Article

Establishment and verification of a predictive model for bone metastasis in patients with non-small cell lung cancer based on peripheral blood CX3CL and CCL28

Shuguang Li[1], Shuai Liu[2], Shanzhou Fang[3], Feifei Zhao[3]

[1]*Department of Radiology, The Fourth Hospital of Hebei Medical University, Shijiazhuang 050011, Hebei, China;* [2]*Department of Orthopaedics, Cangzhou People's Hospital, Cangzhou 061000, Heibei, China;* [3]*Department of Orthopedics, The Fourth Hospital of Hebei Medical University, Shijiazhuang 050011, Hebei, China*

Received March 29, 2024; Accepted May 31, 2024; Epub June 15, 2024; Published June 30, 2024

Abstract: To establish a predictive model of bone metastasis in patients with non-small cell lung cancer (NSCLC) using peripheral blood CX3CL and CCL28, and to verify its application value. We retrospectively gathered clinical data from 210 patients with NSCLC treated at our institution between April 2021 and December 2023. These patients were stratified into two groups based on the presence of bone metastases: a bone metastasis group (n = 49) and a non-bone metastasis group (n = 161). A logistic regression model was developed to predict bone metastasis and to evaluate the model's predictive performance. Multivariate logistic regression analysis identified age (OR = 6.689, P < 0.001), carcinoembryonic antigen (CEA, OR = 5.699, P < 0.001), CX3CL1 (OR = 5.418, P < 0.001), and CCL28 (OR = 7.692, P < 0.001) as independent predictors of bone metastasis in NSCLC patients. The receiver operating characteristic (ROC) curve analysis yielded an area under the curve (AUC) of 0.794 for both the modeling and validation cohorts. Decision curve analysis (DCA) indicated a superior net benefit of the model. Calibration curves confirmed close concordance between predicted and observed probabilities of bone metastasis. The Hosmer-Lemeshow test yielded a chi-square statistic of 4.743 with a *P*-value of 0.178, suggesting a good fit. The predictive model utilizing serum levels of CX3CL1 and CCL28 demonstrates robust predictive accuracy and efficacy for bone metastasis in patients with NSCLC.

Keywords: Non-small cell lung cancer, bone metastasis, CX3 chemokine ligand 1, CC chemokine ligand 28, prediction model

Introduction

Lung cancer is among the most prevalent cancers globally, with non-small cell lung cancer (NSCLC) accounting for roughly 85% of all cases [1]. Distant metastasis poses a substantial threat to the survival of NSCLC patients, with bone metastasis emerging as the predominant form. According to a retrospective analysis, bone metastasis comprises roughly 21.3% of all distant metastatic occurrences in NSCLC patients [2], frequently resulting in disruptions to bone metabolism and skeletal-related events (SREs) like spinal cord compression and pathological fractures. These events profoundly affect patients' quality of life and escalate medical burden. Following the diagnosis of bone metastasis, patients typically have a median survival period of merely 6 to 10 months, and a one-year survival rate ranging from 40% to 50% post-treatment [3]. Therefore, timely prevention and treatment of bone metastasis in NSCLC patients are of paramount importance for improving their prognosis. CX3CL1, the only known member of the CX3C chemokine family, is regulated by a variety of mechanisms. Under normal circumstances, the expression level of CX3CL1 is low, but it can be up-regulated under stimulation such as inflammation and injury. It can bind to the CX3CR1 receptor on the cell surface by adhesion form, thereby mediating intercellular interaction and signal transduction. Previous studies have indicated its involvement in inflammation and various tumor developments [4]. However, its regulatory mechanisms in tumor cell proliferation,

https://doi.org/10.62347/ONRF2499

migration, and invasion in lung cancer patients remain unclear. CCL28 is a chemokine belonging to CC chemokines, also known as mucosal-associated epithelial chemotactic cytokines (MEC). Its expression level is affected by many factors, including pro-inflammatory cytokines, bacterial products, and possible genetic and environmental factors. It mediates cell-to-cell signal transduction by binding to CC chemokine receptor 10 (CCR10) and regulates the migration and activation of immune cells such as macrophages and lymphocytes, participating in mucosal immune response and cell-mediated inflammatory response. Increasing evidence suggests that highly conserved chemokines in evolutionary history are multifunctional molecules, with roles not only in inflammation but also prominently in tumors [5, 6]. This study innovatively integrated peripheral blood levels of CX3CL1 and CCL28 into a nomogram for predicting bone metastasis in NSCLC patients. The findings may offer a useful reference for the clinical management and prevention of bone metastasis in NSCLC patients.

Materials and methods

Study population

This retrospective study analyzed clinical data from 210 patients diagnosed with NSCLC who were admitted to the Fourth Hospital of Hebei Medical University from December 2020 to December 2023. All procedures involving human participants in this study adhered to the ethical standards set by the Ethics Committee of the Fourth Hospital of Hebei Medical University (approval No. 2020ky184) and complied with the 1964 Helsinki Declaration and its subsequent amendments or comparable ethical guidelines.

Inclusion criteria: (1) Diagnosis of NSCLC confirmed by clinical and pathological examination; (2) Age > 18 years; (3) Availability of complete CX3CL1 and CCL28 levels in peripheral blood; (4) Bone metastasis status evaluated by whole-body PET-CT; (5) Availability of complete clinical data. Exclusion criteria: (1) Patients with other concomitant malignant tumors; (2) Patients with comorbidities such as diabetes mellitus or thyroid disorders affecting bone metabolism; (3) Patients with diseases such as osteoporosis or rheumatoid arthritis; (4) Incomplete medical records.

Variables and data collection methods

Study variables: Study variables were primarily categorized into predictive variables and outcome variables. (1) Predictive variables included gender, age, smoking history, comorbidities, pathological type, TNM staging, tumor markers (CEA, reference range of 0~10 μg/L; AFP, reference range of 0~20 μg/L), and alkaline phosphatase (ALP, reference range of 50~136 U/L). Patients' peripheral venous blood samples (5 ml) were procured and anticoagulated using 1.5 mg/ml ethylenediaminetetraacetic acid (EDTA). Subsequently, the samples underwent centrifugation at 3000 rpm for 20 minutes to isolate plasma, which was then stored at -80°C until further analysis. Enzyme-linked immunosorbent assay (ELISA) was employed to quantify peripheral blood levels of CX3CL and CCL28, adhering strictly to the instructions provided by the respective kits (Chemstan, CS103909H)/(ZYscience, H-EL-MEC/CCL28). (2) Outcome variable: Bone metastasis was diagnosed based on bone scintigraphy and clinical symptoms as the gold standard [7].

Diagnostic criteria of bone metastasis: ① Presence of more than 3 sites of radioactive isotope accumulation on bone scintigraphy after excluding benign lesions and other traumatic factors; ② Presence of ≤2 sites of radioactive isotope accumulation on bone scintigraphy along with bone pain, pathological fractures, or other clinical symptoms indicative of bone metastasis; ③ Presence of bone pain, pathological fractures, or other clinical symptoms indicative of bone metastasis with negative results on radioactive isotope examination; ④ Presence of abundant accumulation of radioactive isotopes and clinical symptoms of bone metastasis. Confirmation was based on any of these four criteria.

Data collection: The clinical data of the patients were gathered from electronic medical records, including gender, age, smoking history, basic medical history, pathological type, tumor-lymph node-metastasis (TNM) stage, tumor markers, peripheral blood CX3 CL, CCL28 levels, and bone metastasis status.

Imputation of missing data: To maintain the integrity and accuracy of the data set, this study employed simulation-based imputation for handling missing values. By analyzing correlation in the data before and after the model

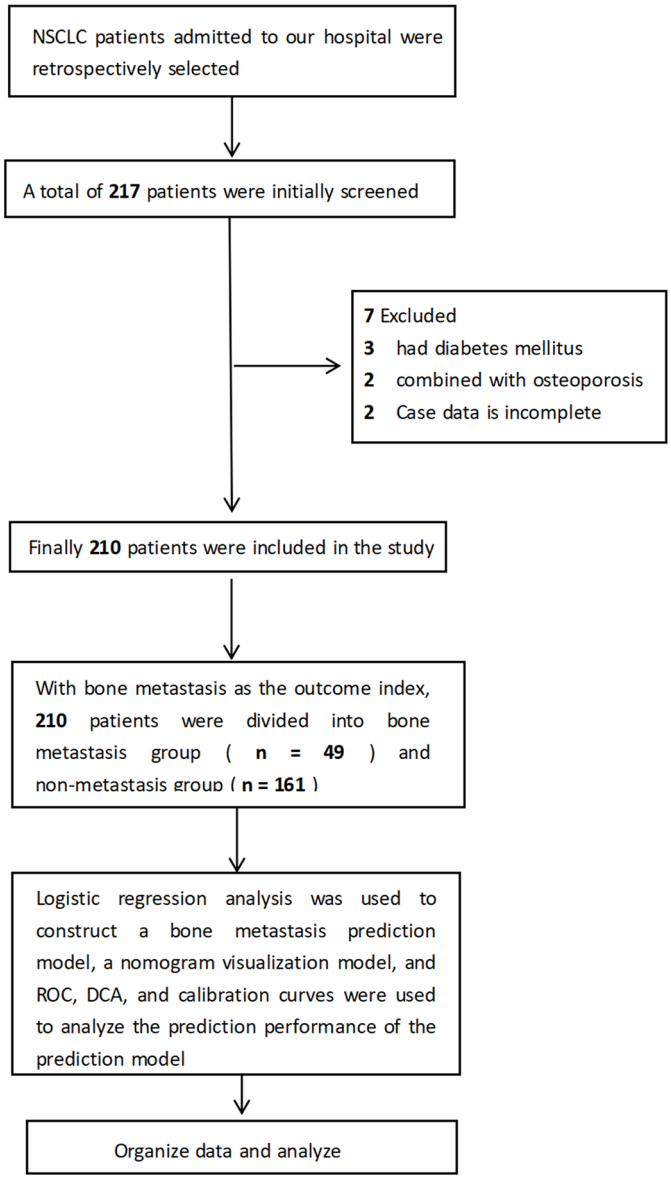

Figure 1. Flow chart.

learning, it was determined that the missing data accounted for 5%, and the missing data values were predicted and filled.

Construction of predictive model

Patients were categorized based on the presence of bone metastasis into a bone metastasis group and a non-bone metastasis group. The cohort employed 100 iterations of 5-fold cross-validation to determine optimal hyperparameters, establish the best training regimen, and validate the model to assess its fit and generalizability. The discrimination of the prediction model was evaluated using the area under the curve (AUC), with higher AUC values indicating better model discrimination. A nomogram was created to visualize the prediction model, where individual variable scores were aggregated to compute a total score reflecting the cumulative contribution of the predictor variables. This total score was then used to determine the corresponding probability of the outcome event by drawing a vertical line from the total score to the probability scale. Model calibration was assessed using a calibration curve and the Hosmer-Lemeshow (H-L) chi-square test, reflecting the agreement between predicted and observed risks across different risk stratifications.

Statistical analysis

Data analysis was performed using R software (version 4.3.1). Continuous data were checked for normality, and the data in normal distribution were presented as mean ± standard deviation, and t-tests were used for comparisons. Categorical data were presented as counts or rates and analyzed using the chi-square test. Risk factors influencing bone metastasis were identified through univariate and multivariate logistic regression analyses. Significant factors in univariate analysis were further analyzed in multivariate logistic regression, taking into account clinical relevance to construct a nomogram prediction model. The ROC curve was plotted, and the AUC was calculated to determine the model's discrimination. The Hosmer-Lemeshow test was used to assess model calibration, and the decision curve analysis (DCA) was employed to evaluate the model's clinical utility. Statistical significance was determined at $P < 0.05$.

Results

Comparison of clinical data between bone metastasis group and non-metastasis group

In a cohort of 210 patients with NSCLC, 49 had bone metastases and 161 did not. The Flow chart is shown in **Figure 1**. Statistical anal-

ysis revealed significant differences between the metastatic and non-metastatic groups in terms of age, pathological type, and levels of CEA, CX3CL1, and CCL28 (all $P < 0.05$), as detailed in **Table 1**.

Multifactor logistic regression analysis of factors influencing bone metastasis in NSCLC patients

Variables that showed significant differences in univariate analysis were used as independent variables. Continuous data such as age, CEA, CX3CL1, and CCL28 were categorized. Multivariate logistic regression, with bone metastasis as the dependent variable, identified age, CEA, CX3CL1, and CCL28 as independent risk factors for bone metastasis in NSCLC patients (all $P < 0.05$). No significant differences were found in other clinical parameters between the two groups (all $P > 0.05$), as shown in **Table 2**.

Establishment and evaluation of the prediction model

The prediction model was developed based on factors that demonstrated statistical differences in multivariate logistic regression analysis. The results of the nomogram model are presented in **Figure 2**. ROC analysis indicated that the model's AUC for predicting bone metastasis in NSCLC patients was 0.794, as illustrated in **Figure 3**. DCA for bone metastasis based on selected risk factors showed a higher net benefit for the prediction model using combined indicators, as shown in **Figure 4**. Calibration curve analysis confirmed good consistency between the predicted and actual occurrences of bone metastasis. The chi-square statistic following the Hosmer-Lemeshow test was 4.743 with a P value of 0.178, as displayed in **Figure 5**.

Discussion

Bone metastasis is a frequent distant site in NSCLC patients. In this study, there were 33 cases of bone metastasis in the modeling group, with an incidence rate of 22.45%. This rate aligns with the results reported by Dohzono S et al. [8], suggesting that clinical attention to the prevention and treatment of bone metastasis in NSCLC patients should still be strengthened. Previous studies have indicated [9, 10] that bone metastasis begins insidiously, with non-specific clinical symptoms, and patients are prone to bone-related adverse events, adversely affecting patients' survival time and quality of life. Therefore, early identification of the high-risk population for bone metastasis is of great significance for improving the prognosis of lung cancer patients. Currently, conventional imaging techniques are commonly used in clinical practice to diagnose bone metastasis, but they also have certain limitations. For example, patients undergo imaging examinations only after manifesting clear symptoms, which is indicative of advanced stage of lung cancer, leading to suboptimal treatment outcomes [11, 12]. There is a need for more accessible and practical methods to predict early bone metastasis in NSCLC patients to enhance patient survival and clinical outcomes, given the economic burden of conventional imaging.

In this study, we investigated 12 potential factors associated with the development of bone metastasis in patients with NSCLC. Single-factor and multifactor logistic regression analyses identified age, CEA, CX3CL1, and CCL28 levels as independent risk factors influencing the occurrence of bone metastasis in NSCLC patients. Some studies have suggested [13] that bone density typically decreases with age, increasing the risk of osteoporosis, which may lead to the occurrence of bone metastasis; meanwhile, aging can also diminish immune function and the body's tolerance for treatments, thus limiting treatment options, and further increasing the risk of bone metastasis [14]. CEA is a tumor marker commonly used to monitor tumor activity. Literature has indicated [15] that elevated CEA level may reflect the invasiveness and malignancy of tumors, increasing the risk of tumor metastasis to the bones. This study underscores the significance of CEA as a sensitive indicator for detecting bone metastasis in lung cancer. The analysis posits CEA as a widely utilized tumor-sensitive marker in clinical practice. CEA is primarily synthesized within the cytoplasm and subsequently secreted into extracellular and surrounding bodily fluids through the cell membrane, rendering it detectable in serum, gastric juice, and other bodily fluids. Notably, as the patient's condition deteriorates, there is a corresponding elevation in CEA levels [16]. Early CEA assessment is routine in the clinical diagnosis of ovarian cancer [17], and prognostic evaluation in cervical can-

Table 1. Comparison of clinical data between bone metastasis group and non-metastasis group

Factors	Bone Metastasis Group (n = 49)	Non-Metastasis Group (n = 161)	χ^2	*P*
Age				
< 60	2	40	10.121	0.002
≥ 60	47	121		
Gender				
Male	30	99	0.001	0.973
Female	19	62		
Smoking history				
Yes	10	37	0.143	0.705
No	39	124		
Medical history				
Yes	18	56	0.063	0.802
No	31	105		
Pathological type				
Adenocarcinoma	44	109	9.273	0.002
Squamous carcinoma	5	52		
T stage				
T_0~T_2	16	64	0.803	0.370
T_3~T_4	33	97		
N stage				
N_0~N_2	27	64	3.605	0.058
N_3 and N_x	22	97		
CEA				
0~10 μg/L	21	114	12.781	0.000
> 10 μg/L	28	47		
AFP				
0~20 μg/L	49	159	0.615	0.433
> 20 μg/L	0	2		
ALP				
< 100 U/L	24	103	3.534	0.060
≥ 100 U/L	25	58		
CX3CL				
< 0.4 pg/mL	3	73	25.021	< 0.001
≥ 0.4 pg/mL	46	88		
CCL28				
< 35 pg/mL	2	78	31.151	< 0.001
≥ 35 pg/mL	47	83		

CEA: carcinoembryonic antigen, AFP: alpha-fetoprotein, ALP: alkaline phosphatase, CX3CL1: CX3 chemokine ligand 1, CCL28: CC chemokine ligand 28.

Table 2. Multifactor logistic regression analysis of factors influencing bone metastasis in NSCLC patients

Factors	*β*	*SE*	Ward χ^2	*P*	*OR*	*95% CI*
Age	1.900	0.457	17.294	< 0.001	6.689	2.731~16.382
Pathological type	0.023	0.089	0.065	0.652	1.023	0.859~1.218
CEA	1.740	0.339	26.354	< 0.001	5.699	2.932~11.075
CX3CL	1.690	0.365	21.431	< 0.001	5.418	2.649~11.080
CCL28	2.040	0.324	39.650	< 0.001	7.692	4.076~14.516

CEA: carcinoembryonic antigen, CX3CL1: CX3 chemokine ligand 1, CCL28: CC chemokine ligand 28.

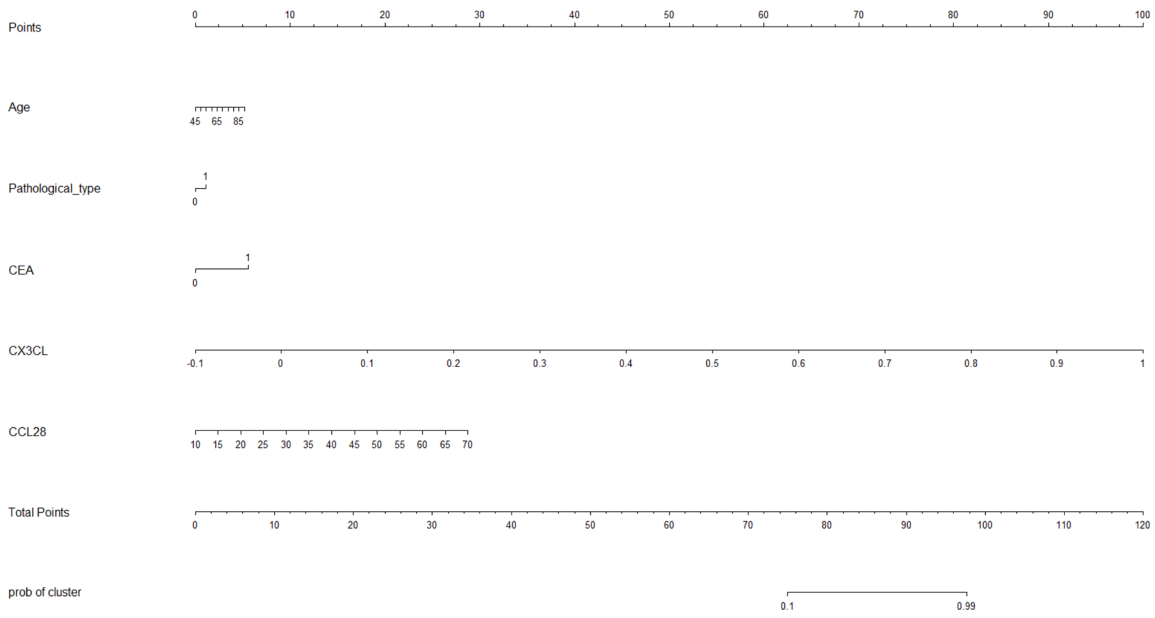

Figure 2. Nomogram model predicting bone metastasis in NSCLC patients.

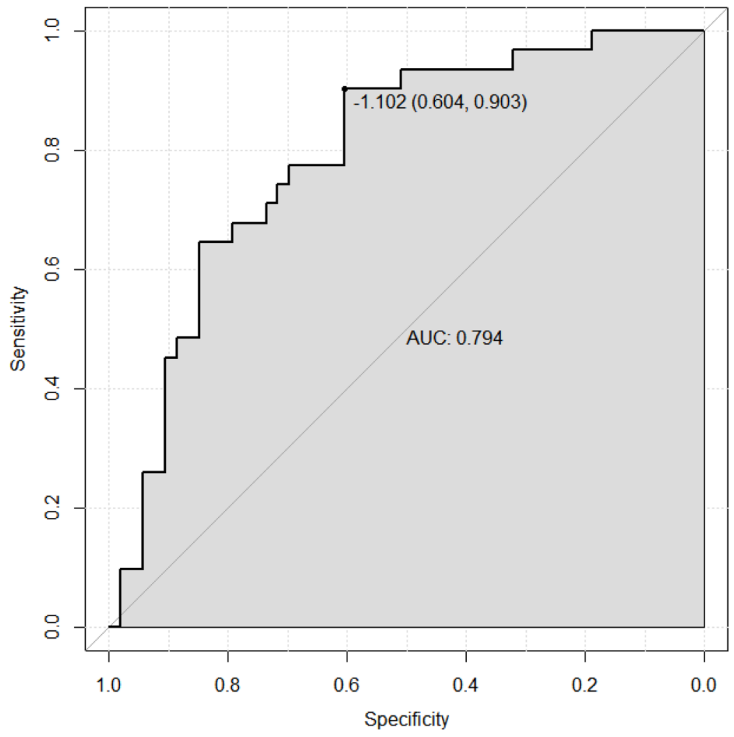

Figure 3. ROC curve of the nomogram model predicting bone metastasis.

cer [18], where it shows high sensitivity and accuracy in predicting disease recurrence.

CX3CL1, also known as neurotactin or fractalkine, is a cytokine crucial for the functioning of both the immune and nervous systems. It primarily functions by binding to its receptor, CX3CR1, to facilitate cell-to-cell signal transduction. This interaction plays a significant role in regulating a variety of biological processes, including inflammation, cell migration, proliferation, and apoptosis. CX3CL1 is vital for neuroprotection within the nervous system as it promotes neuronal survival and supports synaptic transmission [19]. Previous studies have suggested [20, 21] that the CX3CL1/CX3CR1 signaling pathway may be involved in the growth, infiltration, and metastasis of lung cancer. CX3CL1 may affect the migration and invasion ability of lung cancer cells by interacting with CX3CR1 in the tumor microenvironment, thereby affecting the development and metastasis of tumors.

CCL28 is a chemokine that plays an important role in inflammation and immune regulation. Study has found [22] that CCL28 participates in the migration and settlement of lung cancer cells in the microenvironment of bone metasta-

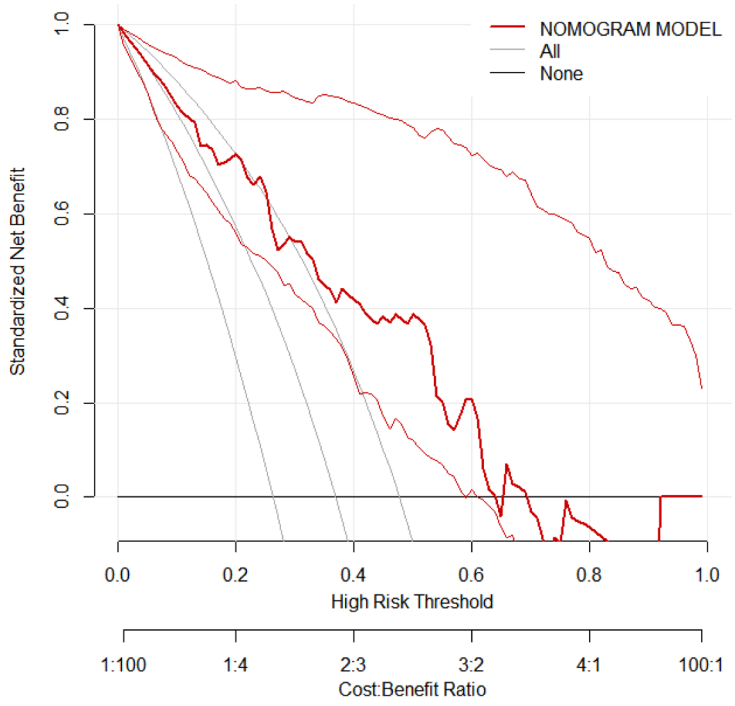

Figure 4. Decision curve analysis (DCA) of the nomogram model predicting bone metastasis.

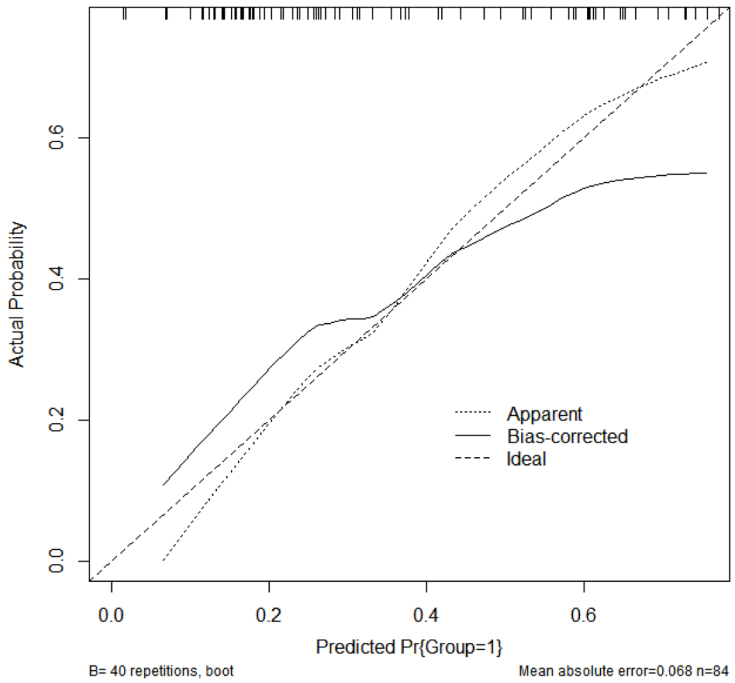

Figure 5. Calibration curve of the nomogram model predicting bone metastasis.

sis, possibly by interacting with specific receptors or cells, affecting the activities of inflammatory cells, immune cells, angiogenesis, and bone remodeling in the bone marrow, thereby affecting the growth and metastasis of lung cancer cells in the bone, increasing the risk of bone metastasis in patients [23].

Nomograms are powerful tools that predict disease risk or survival outcomes by integrating various individual risk factors, quantifying the impact of each variable, and visualizing the results of different patients [24]. In this study, a nomogram predictive model based on age, CEA, CX3CL, and CCL28 levels was constructed using machine learning methods. Machine learning algorithms are adept at handling large datasets, capturing complex patterns and correlations which traditional statistical methods may miss. They improve prediction accuracy through their ability to automatically adjust model parameters and weights, adapt to different data distributions, and manage relationships between features [25, 26]. In this study, the AUC of the nomogram prediction model based on age, CEA, CX3CL, and CCL28 levels to predict bone metastasis in patients was 0.795, and the net benefit of predicting the risk of bone metastasis in NSCLC patients was high. The prediction of bone metastasis has good consistency with the actual occurrence, suggesting that the prediction model based on peripheral blood CX3CL and CCL28 has good efficacy and accuracy in predicting bone metastasis in NSCLC patients, and has good consistency with the actual occurrence.

Conclusions

In summary, the prediction model based on peripheral blood CX3CL and CCL28 has good

efficacy and accuracy in predicting bone metastasis in NSCLC patients and has good consistency with the actual occurrence. The predictive variables identified in this study - age, CEA, CX3CL1, and CCL28 levels - enable medical personnel to swiftly and precisely evaluate the risk of bone metastasis. This investigation is a single-center retrospective study, which presents certain limitations. Future research will involve large-sample, multi-center, and prospective datasets to validate the accuracy of the predictive model.

Disclosure of conflict of interest

None.

Address correspondence to: Feifei Zhao, Department of Orthopedics, The Fourth Hospital of Hebei Medical University, No. 12 Jiankang Road, Shijiazhuang 050011, Hebei, China. E-mail: zhff@hebmu.edu.cn

References

[1] Mithoowani H and Febbraro M. Non-small-cell lung cancer in 2022: a review for general practitioners in oncology. Curr Oncol 2022; 29: 1828-1839.

[2] Adogwa O, Rubio DR, Buchowski JM, D'Souza A, Shlykov MA and Jennings JW. Spine-specific skeletal related events and mortality in non-small cell lung cancer patients: a single-institution analysis. J Neurosurg Spine 2022; 36: 125-132.

[3] Ko HW, Chiu CT, Wang CL, Yang TY, Liu CY, Yu CT, Tseng LC, Kuo CS, Wang CC, Yang MH and Yang CT. Overall survival improvement in patients with epidermal growth factor receptor-mutated non-small cell lung cancer and bone metastasis treated with denosumab. Cancers (Basel) 2022; 14: 3470.

[4] Gong Q, Guo Z, Sun W, Du X, Jiang Y and Liu F. CX3CL1 promotes cell sensitivity to ferroptosis and is associated with the tumor microenvironment in clear cell renal cell carcinoma. BMC Cancer 2022; 22: 1184.

[5] Su X, Wang G, Zheng S, Ge C, Kong F and Wang C. Comprehensive explorations of CCL28 in lung adenocarcinoma immunotherapy and experimental validation. J Inflamm Res 2023; 16: 1325-1342.

[6] Chen J, Xu C, Yang K, Gao R, Cao Y, Liang L, Chen S, Xu S, Rong R, Wang J and Zhu T. Inhibition of ALKBH5 attenuates I/R-induced renal injury in male mice by promoting Ccl28 m6A modification and increasing Treg recruitment. Nat Commun 2023; 14: 1161.

[7] Wang H, Shui L, Chen R, Chen Y, Guo J and Chen Y. Occurrence and prognosis of lung cancer metastasis to major organs: a population-based study. Eur J Cancer Prev 2023; 32: 246-253.

[8] Zhu Z, Yang G, Pang Z, Liang J, Wang W and Zhou Y. Establishment of a regression model of bone metabolism markers for the diagnosis of bone metastases in lung cancer. World J Surg Oncol 2021; 19: 27.

[9] He Y, Luo W, Liu Y, Wang Y, Ma C, Wu Q, Tian P, He D, Jia Z, Lv X, Ma YS, Yang H, Xu K, Zhang X, Xiao Y, Zhang P, Liang Y, Fu D, Yao F and Hu G. IL-20RB mediates tumoral response to osteoclastic niches and promotes bone metastasis of lung cancer. J Clin Invest 2022; 132: e157917.

[10] Bai SB, Cheng Y, Liu DZ, Ji QF, Liu M, Zhang BL, Mei QB and Zhou SY. Bone-targeted PAMAM nanoparticle to treat bone metastases of lung cancer. Nanomedicine (Lond) 2020; 15: 833-849.

[11] Li MP, Liu WC, Sun BL, Zhong NS, Liu ZL, Huang SH, Zhang ZH and Liu JM. Prediction of bone metastasis in non-small cell lung cancer based on machine learning. Front Oncol 2022; 12: 1054300.

[12] Hao Y and Li G. Prediction of distant organ metastasis and overall survival of lung cancer patients: a SEER population-based cohort study. Front Oncol 2023; 13: 1075385.

[13] Jarry U, Bostoën M, Pineau R, Chaillot L, Mennessier V, Montagne P, Motte E, Gournay M, Le Goff A, Guillaudeux T and Pedeux R. Orthotopic model of lung cancer: isolation of bone micro-metastases after tumor escape from Osimertinib treatment. BMC Cancer 2021; 21: 530.

[14] Lin Z, Wang R, Zhou Y, Wang Q, Yang CY, Hao BC and Ke CF. Prediction of distant metastasis and survival prediction of gastric cancer patients with metastasis to the liver, lung, bone, and brain: research based on the SEER database. Ann Transl Med 2022; 10: 16.

[15] Huang F, Cao Y, Wu G, Chen J, CaihongWang, Lin W, Lan R, Wu B, Xie X, Hong J and Fu L. BMP2 signalling activation enhances bone metastases of non-small cell lung cancer. J Cell Mol Med 2020; 24: 10768-10784.

[16] Ren L and Yang Y. Value of dual-source CT dual-energy parameters combined with serum detection of VEGF and CEA in the diagnosis of early lung cancer. Biotechnol Genet Eng Rev 2023; [Epub ahead of print].

[17] Li M, Tan J, Zhang Y, Ai C, Wang H, Zhang H, Jin Y and Chen Y. Assessing CT imaging features combined with CEA and CA125 levels to identify endometriosis-associated ovarian cancer. Abdom Radiol (NY) 2021; 46: 2367-2375.

[18] Liu Y, Shi L, Chen K and Ye W. Identification and validation of serum tumor-markers based nomogram to predict the prognostic value of patients with cervical adenocarcinoma. Curr Probl Cancer 2022; 46: 100899.
[19] Subbarayan MS, Joly-Amado A, Bickford PC and Nash KR. CX3CL1/CX3CR1 signaling targets for the treatment of neurodegenerative diseases. Pharmacol Ther 2022; 231: 107989.
[20] Que ZJ, Yao JL, Zhou ZY, Yu P, Luo B, Li HG, Liu JX, Xu HX and Tian JH. Jinfukang inhibits lung cancer metastasis by upregulating CX3CL1 to recruit NK cells to kill CTCs. J Ethnopharmacol 2021; 275: 114175.
[21] Tang W, Jia P, Zuo L and Zhao J. Suppression of CX3CL1 by miR-497-5p inhibits cell growth and invasion through inactivating the ERK/AKT pathway in NSCLC cells. Cell Cycle 2022; 21: 1697-1709.
[22] Lin D, Zhang M, Guo H, Deng Y, Zhong B, Liao F and Xu Z. Dispensable role of CCL28 in Kras-mutated non-small cell lung cancer mouse models. Acta Biochim Biophys Sin (Shanghai) 2020; 52: 691-694.
[23] Liu B and Wei C. Hypoxia induces overexpression of CCL28 to recruit treg cells to enhance angiogenesis in lung adenocarcinoma. J Environ Pathol Toxicol Oncol 2021; 40: 65-74.
[24] Tian Z, Li C, Wang X, Sun H, Zhang P and Yu Z. Prediction of bone metastasis risk of early breast cancer based on nomogram of clinicopathological characteristics and hematological parameters. Front Oncol 2023; 13: 1136198.
[25] Fan TD, Bei DK and Li SW. Nomogram models based on the gene expression in prediction of breast cancer bone metastasis. J Healthc Eng 2022; 2022: 8431946.
[26] Xu Y, Wu H, Xu G, Yin Z, Wang X, Chekhonin VP, Peltzer K, Li S, Li H, Zhang J, Ma W and Zhang C. Survival estimation, prognostic factors evaluation, and prognostic prediction nomogram construction of breast cancer patients with bone metastasis in the department of bone and soft tissue tumor: a single center experience of 8 years in Tianjin, China. Breast J 2022; 2022: 7140884.